

Resonant-Wavelength Tuning of Microring Filters by Oxygen Plasma Treatment

Tzyy-Jiann Wang, *Member, IEEE*, Yen-Hao Huang, and Hsuen-Li Chen

Abstract—The resonant-wavelength tuning of integrated-optic microring filters in silicon nitride using oxygen plasma treatment is demonstrated. During the treatment, high-energy oxygen ions in the plasma enter into the device surface such that the material composition is converted to SiO_xN_y . The corresponding index variation results in a modification of the effective index of the guide mode and, therefore, the tuning of the resonant wavelength of microring filters. The effects of treatment parameters, such as radio-frequency power, oxygen flow rate, and treatment time, on the characteristics of microring filters are discussed. Experimental results show that the resonant wavelengths of microring filters can be effectively tuned over a range larger than their free spectral ranges.

Index Terms—Integrated optics, microring filter, wavelength tuning.

I. INTRODUCTION

INTEGRATED-OPTIC microring resonators are promising components in optical integrated circuit. The excellent wavelength-selective characteristics in a micrometer structure make them widely applied in many passive and active devices. Various advanced applications, such as wavelength notch filtering, dispersion compensation, wavelength add-drop for dense wavelength-division multiplexing, semiconductor ring laser, and wavelength conversion have been demonstrated. In experiments, they are successfully fabricated in different material systems, which include silica on silicon [1], silicon nitride (SiN) on silica [2], silicon on insulator [3], GaAs–AlGaAs [4], and GaInAsP–InP [5]. The resonant wavelength of microring resonators is determined by the effective index of the guide modes and the ring radius in the waveguide structure. Due to its high sensitivity to these two parameters, the slight deviation of material composition and dimensional parameters from the design affects these two parameters, and results in a remarkable variation of the resonant wavelength. Because the accuracy in the present device fabrication is insufficient, the postfabrication wavelength tuning is unavoidable in order to obtain the desired spectral characteristics. In previous research, overlay index tuning by ultraviolet illumination [6] and temperature control during device operation [7]–[9] are proposed to tune statically the resonant wavelength of microring filters. The former has the problem of incompatibility to the standard semiconductor

Manuscript received July 1, 2004; revised October 6, 2004. This work was supported by the National Science Council, Taipei, Taiwan, R.O.C., under Contract NSC 93-2215-E-027-010.

T.-J. Wang and Y.-H. Huang are with the Institute of Electro-Optical Engineering, National Taipei University of Technology, Taipei 10651, Taiwan, R.O.C. (e-mail: f10939@ntut.edu.tw).

H.-L. Chen is with the National Nano Device Laboratories, Hsinchu 30050, Taiwan, R.O.C.

Digital Object Identifier 10.1109/LPT.2004.840921

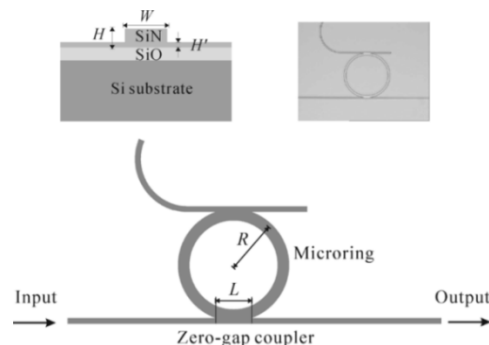


Fig. 1. Top view of integrated-optic microring filter. (Inset: (upper-left) SiN ridge waveguide structure; (upper-right) photograph of the fabricated microring filter).

fabrication process. The latter can be applied in both of the static and dynamic wavelength tuning. In this work, oxygen plasma treatment is proposed to tune the resonant wavelength of microring filters fabricated in SiN on the silicon substrate. The effects of treatment parameters, such as radio-frequency (RF) power, oxygen flow rate, and treatment time on the spectral characteristics of microring filters are discussed.

II. PRINCIPLE OF WAVELENGTH TUNING

Fig. 1 shows the top view of integrated-optic microring filter with the SiN ridge waveguide structure. The ridge waveguide, whose structure is shown in the upper-left inset of Fig. 1, is formed on the silicon substrate and has the waveguide layer with $H = 0.48 \mu\text{m}$ and $H' = 0.06 \mu\text{m}$. The air and the $4\text{-}\mu\text{m}$ -thick silica layer are used as the upper- and the lower-cladding layers. The microring filter consists of $1\text{-}\mu\text{m}$ -wide input–output waveguides and a ring waveguide with the waveguide width of $2.5 \mu\text{m}$ and the ring radius $R = 25 \mu\text{m}$. The ring waveguide is widened in order to increase the optical confinement and reduce the propagation loss in the ring waveguide. At the intersection of the straight and the ring waveguides, the zero-gap coupler with the coupler length $L = 4 \mu\text{m}$ is used in order to reduce the effect of the etching depth on the coupling coefficient. The microring filter is designed to filter out the specific wavelength in the input light, which is equal to the resonant wavelength of the microring filter.

The fabrication process of microring filters is described as follows. First, the silica layer is formed on the p-type $\langle 100 \rangle$ silicon substrate by plasma-enhanced chemical vapor deposition (PECVD) using tetraethoxysilane of 10 sccm and oxygen gas of 400 sccm with the pressure of 300 mtorr and the RF power of 200 W. Then the SiN layer is deposited by PECVD using SiH_4 of 20 sccm and NH_3 of 80 sccm with the pressure of 500 mtorr and the RF power of 50 W. During the deposition process, the

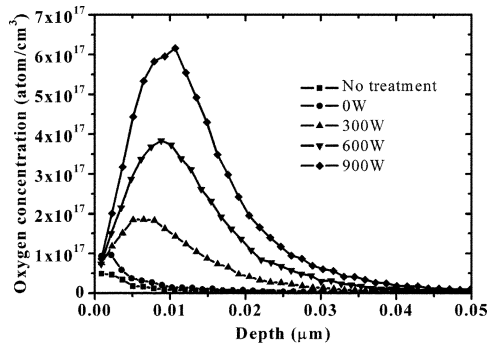


Fig. 2. Oxygen concentration distribution in the SiN layer without plasma treatment and after plasma treatment for the RF power of 0, 300, 600, and 900 W with the oxygen flow rate of 800 sccm and the treatment time of 10 min.

hydrogen ions are incorporated into the film and form the N–H and Si–H bonds, whose vibrational overtones result in the optical absorption around the wavelength of 1500 nm. Besides, the hydrogen ions in SiN give rise to the instability of film composition. In order to remove the hydrogen ions in the SiN film, this film is processed by rapid thermal annealing at 900 °C for 120 s. After rapid thermal annealing, the optical absorption around 1500 nm disappears in the Fourier transform infrared spectroscopy. In addition, the film roughness measured by atomic force microscope is improved and the SiN film becomes denser. The pattern of microring filters is transferred to the photoresist on the silicon substrate by e-beam lithography. The patterned photoresist is used as the protective layer in the sequential etching process. The RIE system using CHF₃ at a flow rate of 40 sccm and CF₄ at a flow rate of 80 sccm with the RF power of 90 W is used to etch the SiN layer to form the device structure.

The oxygen plasma treatment is carried out in the PECVD system. During the process of oxygen plasma treatment, high-energy oxygen ions enter into the material and the material composition on the device surface is converted to silicon oxynitride (SiO_xN_y), whose composition ratio is related to the condition of plasma treatment. The refractive index of SiO_xN_y thin films is dependent on the incorporation quantity of oxygen in the SiN layer and can be tuned over a large range between 1.45 (SiO₂) and 2.0 (Si₃N₄). Because the index of silicon oxynitride is smaller than that of SiN, the oxygen plasma treatment produces a waveguide structure, whose index distribution is varied. The resonance condition for the microring filter is $(2\pi \cdot r + 2 \cdot l) \cdot n_{\text{eff}} = m \cdot \lambda_m$, where r is the ring radius, l is the coupler length, n_{eff} is the effective index of the guide mode in the ring waveguide, m is an integer, and λ_m is the resonance wavelength of order m . The free spectral range (FSR) expressed in wavelength is $\Delta\lambda = \lambda^2 / [(2\pi \cdot r + 2 \cdot l) \cdot n_{\text{eff}}]$. Because the oxygen plasma treatment decreases the effective index of the guide mode, the resultant resonant wavelength is blue-shifted and the free spectral range expressed in wavelength becomes larger.

III. EXPERIMENT AND RESULTS

The effects of RF power and heating in the flowing oxygen gas on the concentration distribution of oxygen ions in the SiN layer are first investigated. The sample for studying the effect of oxygen plasma treatment has the same layers as that for fabricating the microring filters. The oxygen concentration distribution is analyzed by secondary ion mass spectroscopy. Fig. 2

shows the oxygen concentration distribution in the SiN layer before and after oxygen plasma treatment. The RF power to be applied is 0, 300, 600, and 900 W. Because the substrate is heated to the temperature of 300 °C during the process of oxygen plasma treatment, the case for the RF power of 0 W is used to consider the heating effect on the oxygen concentration distribution. For the sample without plasma treatment, the appearance of a small quantity of oxygen on the surface of the SiN layer is due to the exposure of the substrate in the air. As the substrate is put in the oxygen flow at 300 °C (corresponding to the case for the RF power of 0 W), the oxygen concentration at the interface between air and SiN layer is doubled. The depth of the concentration distribution has no obvious change due to low treatment temperature. When the applied RF power gradually increases, the kinetic energy of the incident oxygen ions becomes larger and the oxygen concentration distribution presents an obvious change. For the sample treated by the oxygen plasma with the RF power of 200 W and the treatment time of 2 min, the oxygen distribution concentration has a maximal value at the surface and a depth of 0.02 μm. In order to have a larger depth in the oxygen concentration distribution, the applied RF power is increased to 300, 600, and 900 W. It is noted that, as the RF power is larger than 300 W, the oxygen concentration distribution has a Gaussian-like distribution with a concentration maximum beneath the surface of the SiN layer, which is different from the case for the RF power of 200 W with a concentration maximum at the surface. It is a result of high kinetic energy of incident oxygen ions with the similar formation mechanism as ion implantation. Besides, as the RF power increases, the maximum concentration grows linearly at a rate of 7.18×10^{14} atom/(cm³ · W) and the peak depth also increases linearly with the RF power at a rate of 6.97×10^{-6} μm/W. The depths corresponding to the oxygen concentration of 1×10^{16} atom/cm³ are 0.032, 0.041, and 0.051 μm for the RF power of 300, 600, and 900 W, respectively. In the characteristics measurement of microring filters, the laser light from a tunable external-cavity semiconductor laser with a tunable wavelength range of 1580~1600 nm is butt-coupled into the waveguide. The output light from the microring filter is collected by 40× objective lens, and a wavelength-calibrated optical power meter is used to measure its output power. The microring filter before oxygen-plasma treatment has the resonant wavelength at 1591.3 nm.

The effects of oxygen plasma treatment parameters on the spectral characteristics of microring filters for transverse-electric (TE) polarization are presented. Fig. 3 shows the spectral characteristics of microring filters in the output port for the RF power of 300, 600, and 900 W. As the RF power increases, the resonant wavelength linearly shifts to the shorter wavelength at a rate of -9.73×10^{-3} nm/W. Their resonant wavelengths are 1588.4, 1585.9, and 1582.4 nm for the RF power of 300, 600, and 900 W, respectively. Their corresponding FSRs are 8.0, 8.2, and 8.4 nm. The larger the RF power, the more energy the incident oxygen ions have, and the more oxygen ions enter into the device and reach a deeper position. The higher oxygen concentration and the deeper distribution in the waveguide structure result in a depressed effective index and, therefore, a blue shift of the resonant wavelength. As the RF power increases to 900 W, the resonant wavelength is tuned over the

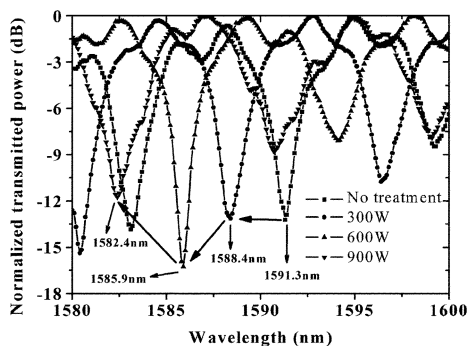


Fig. 3. Output spectra of microring filters without plasma treatment and after plasma treatment for the RF power of 300, 600, and 900 W with the treatment time of 10 min and the oxygen flow rate of 800 sccm.

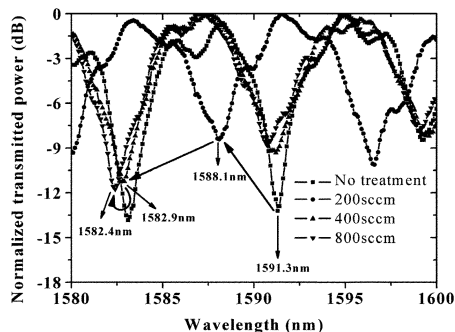


Fig. 4. Output spectra of microring filters without plasma treatment and after plasma treatment for the oxygen flow rate of 200, 400, and 800 sccm with the RF power of 900 W and the treatment time of 10 min.

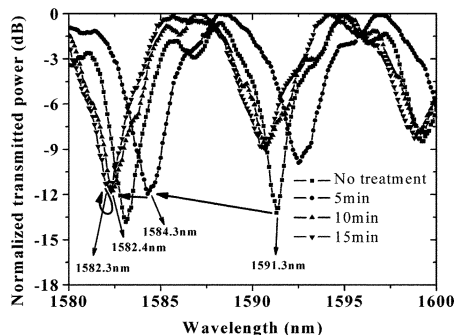


Fig. 5. Output spectra of microring filters without plasma treatment and after plasma treatment for the treatment time of 5, 10, and 15 min with the RF power of 900 W and the oxygen flow rate of 800 sccm.

range of 8.9 nm, which is larger than the FSR value of the microring filter. Fig. 4 shows the spectral characteristics of microring filters in the output port for the oxygen flow rate of 200, 400, and 800 sccm. The larger the oxygen flow rate, the more oxygen ions are incident on the device in a unit time. The resonance of these microring resonators occurs at the wavelength of 1588.1, 1582.9, and 1582.4 nm for the oxygen flow rate of 200, 400, and 800 sccm, respectively. The resonant wavelength can be tuned over the range of 8.9 nm. As the oxygen flow rate increases to about 400 sccm, the number of incoming oxygen ions into the device tends to be saturated, and the variation of the effective mode index with the oxygen flow rate is reduced. Hence, the corresponding resonant-wavelength shift becomes smaller. The corresponding FSRs are 8.0, 8.3, and 8.4 nm. Fig. 5 shows the spectral characteristics of microring

filters in the output port for the treatment time of 5, 10, and 15 min. The corresponding resonant wavelengths are 1584.3, 1582.4, and 1582.3 nm. The resonant wavelength tuning is more effective in the treatment-time range of 0~5 min with a tuning range of 7 nm. Therefore, the oxygen plasma treatment can be used for rapid wavelength tuning of microring filters. The variation of minimum transmitted power is due to the effect of oxygen plasma treatment on the coupling coefficient of the zero-gap coupler. Because the resultant index change by plasma treatment is small, the power reflection due to the index discontinuity and, thus, its effect on the device performance can be ignored.

IV. CONCLUSION

A new wavelength tuning technique for integrated-optic microring filters using oxygen plasma treatment has been successfully demonstrated. Exposure of the device surface to the irradiation of high-energy oxygen plasma can modify the material composition from SiN to silicon oxynitride (SiO_xN_y), whose composition ratio is dependent on the treatment condition. The incorporation of oxygen ions into the SiN layer reduces the effective index of the guided mode such that the resonant wavelengths of microring filters are blue-shifted and the FSRs expressed in wavelength become larger. The effects of plasma treatment parameters, such as RF power, oxygen flow rate, and treatment time, on the spectral characteristics of microring filter are considered in this work. Experimental results show that the resonant wavelength can be effectively tuned over the range of 8.9 nm, which is larger than the FSR value. The proposed method has the advantages of large wavelength-tuning range, rapid wavelength tuning, and fabrication compatibility with the standard semiconductor fabrication process.

REFERENCES

- [1] R. Adar, Y. Shani, C. H. Henry, R. C. Kistler, G. E. Blonder, and N. A. Olsson, "Measurement of very low-loss silica on silicon waveguides with a ring resonator," *Appl. Phys. Lett.*, vol. 58, no. 5, pp. 444–445, Feb. 1991.
- [2] D. J. W. Klunder, F. S. Tan, T. van der Veen, H. F. Bulthuis, H. J. W. M. Hockstra, and A. Driessen, "Design and characterization of waveguide-coupled cylindrical microring resonators in Si_3N_4 ," in *IEEE LEOS Annu. Meeting*, 2000, pp. 758–759.
- [3] B. E. Little, J. S. Foresi, G. Steinmeyer, E. R. Thoen, S. T. Chu, H. A. Haus, E. P. Ippen, L. C. Kimerling, and W. Greene, "Ultra-compact Si-SiO₂ microring resonator optical channel dropping filters," *IEEE Photon. Technol. Lett.*, vol. 10, no. 4, pp. 549–551, Apr. 1998.
- [4] D. Rafizadeh, J. P. Zhang, S. C. Hagness, A. Taflove, K. A. Stair, S. T. Ho, and R. C. Tiberio, "Waveguide-coupled AlGaAs/GaAs microcavity ring and disk resonators with high finesse and 21.6 nm free spectral range," *Opt. Lett.*, vol. 22, no. 16, pp. 1244–1246, Aug. 1997.
- [5] D. G. Rabus, M. Hamacher, U. Troppenz, and H. Heidrich, "High-Q channel-dropping filters using ring resonator with integrated SOAs," *IEEE Photon. Technol. Lett.*, vol. 14, no. 10, pp. 1442–1444, Oct. 2002.
- [6] S. T. Chu, W. Pan, S. Sato, T. Kaneko, B. E. Little, and Y. Kokubun, "Wavelength trimming of a microring resonator filter by means of a UV sensitive polymer overlay," *IEEE Photon. Technol. Lett.*, vol. 11, no. 6, pp. 688–690, Jun. 1999.
- [7] D. Rafizadeh, J. P. Zhang, S. C. Hagness, A. Taflove, K. A. Stair, and S. T. Ho, "Temperature tuning of microcavity ring and disk resonators at 1.5 μm ," in *IEEE LEOS 10th Annu. Meeting*, 1997, pp. 162–163.
- [8] P. Katila, P. Hcimala, and J. Arnio, "Thermo-optically controlled ring resonator on silicon," *Electron. Lett.*, vol. 32, no. 11, pp. 1005–1006, May 1996.
- [9] P. Rabiei and W. H. Steier, "Tunable polymer double micro-ring filters," *IEEE Photon. Technol. Lett.*, vol. 15, no. 9, pp. 1255–1257, Sep. 2003.